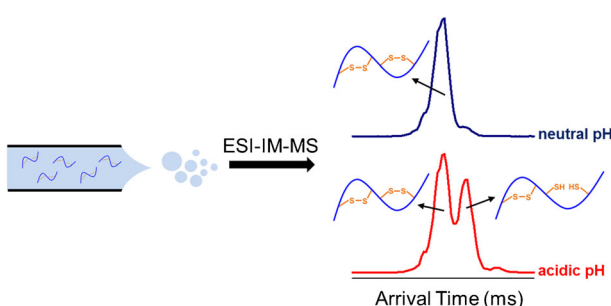


RESEARCH ARTICLE

In-Source Reduction of Disulfide-Bonded Peptides Monitored by Ion Mobility Mass Spectrometry

Bradley B. Stocks, Jeremy E. Melanson

National Research Council of Canada, Measurement Science and Standards, 1200 Montreal Road, Ottawa, ON K1A 0R6, Canada



Abstract. Many peptides with antimicrobial activity and/or therapeutic potential contain disulfide bonds as a means to enhance stability, and their quantitation is often performed using electrospray ionization mass spectrometry (ESI-MS). Disulfides can be reduced during ESI under commonly used instrument conditions, which has the potential to hinder accurate peptide quantitation. We demonstrate that this in-source reduction (ISR) is predominantly observed for peptides in-

fused from acidic solutions and subjected to elevated ESI voltages (3–4 kV). ISR is readily apparent in the mass spectrum of oxytocin—a small, single disulfide-containing peptide. However, subtle m/z shifts due to partial ISR of highly charged ($z \geq 3$) peptides with multiple disulfide linkages may proceed unnoticed. Ion mobility (IM)-MS separates ions on the basis of charge and shape in the gas phase, and using insulin as a model system, we show that IM-MS arrival time distributions (ATDs) are particularly sensitive to partial ISR of large peptides. Isotope modeling allows for the relative quantitation of disulfide-intact and partially reduced states of the mobility-separated peptide conformers. Interestingly, hepcidin peptides ionized from acidic solutions at elevated ESI voltages undergo gas-phase compaction, ostensibly due to partial disulfide ISR. Our IM-MS results lead us to propose that residual acid is the likely cause of disparate ATDs recently measured for hepcidin from different suppliers [Anal. Bioanal. Chem. **409**, 2559–2567 (2017)]. Overall, our results demonstrate the utility of IM-MS to detect partial ISR of disulfide-bonded peptides and reinforce the notion that peptide/protein measurements should be carried out using minimally activating instrument conditions.

Keywords: Peptide, Disulfide bond, In-source reduction, Ion mobility mass spectrometry

Received: 19 October 2017/Revised: 15 January 2018/Accepted: 18 January 2018/Published Online: 15 February 2018

Introduction

Peptide therapeutics offer a compromise between the high selectivity of biologics and the ease of administration of small-molecule drugs, and are thus forecast to garner increased market share in the coming years [1]. Therapeutic peptides have historically been hampered by poor bioavailability due to rapid protease degradation. Intra-peptide cross-linking, or stapling, can increase the half-life of therapeutic peptides by

many fold depending on the number and location of staples [2]. Disulfide bonds between cysteine residues are natural cross-links that impart stability to polypeptide chains [3, 4] and can prolong the lifetime of therapeutic peptides in vivo [5]. Disulfides link immunoglobulin chains as well as constrain the structure of many peptides with therapeutic or antimicrobial activity [6], and the abundance of peptide therapeutics containing disulfide bonds currently in preclinical studies or clinical trials speaks to the importance of this post-translational modification [7]. Consequently, having the ability to structurally characterize and accurately quantify disulfide-containing peptides is crucial.

Proteomics relies on the accurate identification and quantitation of peptides by mass spectrometry (MS). Sequencing

Electronic supplementary material The online version of this article (<https://doi.org/10.1007/s13361-018-1894-1>) contains supplementary material, which is available to authorized users.

Correspondence to: Bradley Stocks; e-mail: bradley.stocks@nrc-cnrc.gc.ca

disulfide-containing peptides by tandem MS can be challenging due to a reduced number of collision-induced fragment ions observed in the spectrum. Typical proteomics workflows therefore incorporate time-consuming chemical disulfide reduction and cysteine alkylation steps to improve sequence coverage [8]; however, disulfide linkage information is lost in the process. Methodology for cleaving disulfides in the mass spectrometer, such as oxidative breakage with plasma [9] or UV irradiation [10], as well as cationization with metal ions [11], can be found in the literature. These techniques allow for much greater structural information to be gleaned from the peptide fragmentation spectra. Online disulfide reduction has become prevalent due to commercialization of a small electrochemical cell that can easily be incorporated between the liquid chromatograph (LC) and the MS [12], facilitating the structural analysis of large disulfide-linked proteins such as monoclonal antibodies [13, 14]. Recently, an in-source reduction (ISR) approach has been reported that does not rely on an external electrochemical cell, but rather on electrospray ionization (ESI) voltage [13, 15]. Because ISR is only observed under elevated ESI capillary voltages, it is postulated to be the result of corona discharge [15]. While protein modifications are known to occur under corona discharge conditions [16, 17], the exact mechanism of ISR remains to be elucidated.

Ion mobility mass spectrometry (IM-MS) has become an indispensable tool for monitoring protein conformation [18–24]. It is generally accepted that large protein complexes retain their solution phase structure upon introduction into the gas phase [25], but the story is not as clear for non-globular and partially denatured species [26, 27]. The gas-phase structure of a polypeptide is largely determined by its charge state, and electrostatic repulsion within a charge-dense sequence tends to favor the formation of extended structures. In addition to increasing peptide identifications in proteomics experiments by reducing spectral overlap [28], IM is useful for interrogating peptide conformational changes. Clemmer and coworkers employed IM-MS to demonstrate that the nonapeptide bradykinin populates multiple conformations dependent on solution conditions and the configurations of its three proline residues [29, 30]. Conformational separation of peptides containing isomeric disulfide linkages has also been achieved with IM-MS [31]. Due to the fact that peptides and proteins can possess higher-order structure, the notion of conformational purity has recently been introduced in the characterization of protein reference materials [32]. IM-MS plays a critical role in assessing higher-order structure as it can detect conformational changes that may not be observable by conventional LC-MS. A recent investigation found that the disulfide-containing potential therapeutic peptide hepcidin synthesized via distinct pathways exhibited dramatically different ion mobility profiles, suggesting that while the final samples may be chemically equivalent, the higher-order structure of peptides and/or proteins can be affected by the manner in which they are produced [33].

This work explores solution conditions and instrument parameters that are crucial to the occurrence of ISR of disulfide-bonded peptides. Previous reports of ISR observed the phenomenon at elevated capillary voltages and found enhanced ISR at low concentrations of organic modifier, however did not address solution pH. Our results show that disulfide ISR is dependent on both solution pH and ESI voltage. While disulfide breakage is negligible when peptides are infused from neutral solution, reduction is prevalent when analyzing acidic solutions. In addition, the magnitude of ISR is increased at elevated ESI capillary voltages. It is demonstrated that disulfide reduction does not appreciably change the conformation of the small, doubly charged peptide oxytocin, but rather its mass spectrum offers clear insight into the occurrence of ISR. Alternatively, for larger and more highly charged peptides such as insulin and hepcidin, the mass spectra show subtle changes upon ISR, whereas the ion mobility arrival time distributions (ATDs) show marked differences in the peptide conformational ensemble. Insulin is a heterodimeric peptide, with its chains linked by two disulfide bonds. It undergoes a conformational expansion as its disulfide bonds become partially reduced, and complete reduction is monitored through the accumulation of isolated A- and B-chains. Alternatively, hepcidin experiences a conformational compaction after partial ISR. Overall, our data show that IM-MS is a valuable technique to monitor ISR of large, highly charged peptides, and minimizing instrument voltages and temperatures can alleviate potential concerns of solution inconsistencies.

Experiment

Chemicals and Reagents

Ammonium acetate and LC-MS grade formic acid were obtained from Fisher Scientific (Nepean, ON). Dithiothreitol (DTT) and bovine insulin were purchased from Sigma (St. Louis, MO). Human hepcidin with the four endogenous disulfide bridges intact [34] was from AnaSpec (Fremont, CA), and oxytocin was from the U.S. Pharmacopeia (Rockville, MD). A NRC candidate certified reference material (CRM) for angiotensin II (AngII) was used to assess the reproducibility of IM measurements. Deionized water (18 M Ω) was produced in-house with a Barnstead Nanopure system (ThermoFisher Scientific, San Jose, CA).

Ion Mobility Mass Spectrometry and Data Analysis

Peptides were dissolved to 1–5 μ M in 10 mM ammonium acetate at pH 6.8, or adjusted to pH 2.6 with formic acid. Reduced oxytocin and hepcidin samples were prepared via 1-h incubations with 50 mM DTT at 60 °C. All peptide solutions were infused at 5 μ L min⁻¹ using a syringe pump (Harvard Apparatus, South Natick, MA) into the ESI source of a Waters (Milford, MA) Synapt G2 Q-TOF mass spectrometer operating in positive ionization mode. To avoid gas-phase activation of the biomolecules, instrument voltages and temperatures were

minimized while still allowing for analyte signal to be observed [27]. Briefly, the capillary voltage was operated between 2 and 4.5 kV while the cone and extraction cone voltages were kept at 20 and 2 V, respectively. The ion source block was maintained at 25 °C and the desolvation gas was heated to 40 °C. The IMS traveling-wave ion guide (TWIG) wave velocity was set to 800 m s⁻¹ with a wave height of 40 V. The IMS gas flow was 90 mL min⁻¹ N₂, resulting in a pressure reading of ~3 mbar. These settings maximized the number of mobility bins used while minimizing carryover between pulses. The transfer TWIG wave velocity and wave height were operated at 268 m s⁻¹ and 4 V, respectively, while the source and trap TWIGs were controlled automatically. In replicate analyses, arrival times were found to be reproducible to <0.1 ms. Calibration of the ion mobility cell was carried out with 10 μM poly-D,L-alanine (Sigma) dissolved in 49.5/49.5/1 water/methanol/acetic acid. Arrival time distributions and mass spectra were extracted using MassLynx 4.1 software from the instrument manufacturer, and conversion to collision cross section (CCS) was accomplished using published polyalanine CCS values measured in N₂ buffer gas [35]. Theoretical peptide isotopologue *m/z* values and relative abundances for native, partially reduced, and reduced peptides were determined with ProteinProspector [36]; each disulfide reduction increased by two the number of hydrogens in the peptide molecular formula. Non-linear least squares fitting was performed via the Solver routine in Microsoft Excel 2010. Average disulfide fractions and standard deviations were calculated from triplicate measurements.

Results and Discussion

Oxytocin Conformation Monitored by ESI-IM-MS

Ion mobility measurements reveal that the gas-phase conformation of doubly charged oxytocin (OT) is minimally affected by solution pH or ESI capillary voltage (Fig. 1a–c). This is perhaps unsurprising considering OT is a nearly cyclic peptide; it contains nine residues with a disulfide linkage between Cys¹ and Cys⁶ (Fig. S1). The Pro⁷-Leu⁸-Gly⁹ tail is highly flexible in aqueous solution [37]; thus, further gas-phase activation is not anticipated. Additional interrogation of the ATDs reveal that a slight shift to longer time occurs for OT infused from acidic solution, perhaps indicating a small conformational expansion. To assess the validity of this interpretation, we analyzed angiotensin II (AngII), an 8-residue peptide containing no cysteine residues, under the same conditions used for OT. Figure S2 shows that, regardless of solution pH or capillary voltage, the [AngII+2H]²⁺ arrival times are consistent within ±0.07 ms or ±1 mobility bin for the applied instrument settings. We therefore considered arrival time differences ≥0.14 ms to be significant, and thus, for the purpose of this study, the OT ATDs shown in Fig. 1a–c are indistinguishable.

While OT conformation appeared insensitive to both capillary voltage and solution pH, these parameters greatly affected the observed mass spectra (Fig. 1d–f). Minimal voltage-

dependent differences are seen when the peptide is infused from neutral solution; however, electrospraying at elevated voltages from an acidic medium causes a distortion to higher *m/z*. While solution pH does not affect the isotopic envelope under gentle ionization conditions (Fig. 1d), enhanced signal response is observed for all peaks beginning with the *M* + 2 isotopologue when the ESI capillary is increased to 3 kV and above (Fig. 1e, f). This implies that a fraction of the OT population undergoes a +2 Da modification during ionization, suggestive of disulfide bond reduction (S-S + 2 H⁺ + 2 e⁻ → 2 SH).

Corona discharge occurs at elevated ESI spray voltages and can result in protein oxidation due to hydroxyl radicals, manifesting as +16 Da increases in the mass spectrum [16, 17]. Figure S3 shows that OT does become oxidized to a small extent when sprayed at 4 kV; however, this does not explain the +2 Da shift observed in Fig. 1e, f. Previous reports indicate that disulfide bonds can be oxidatively cleaved during ESI, for example, through interaction with a plasma [9] or ultraviolet irradiation [10], to form a thiol (-SH) and a sulfinyl radical (-SO·), but this results in a +17-Da mass increase for peptides containing an intra-chain disulfide. Alternatively, it has recently been shown that disulfide reduction occurs under certain ESI conditions [13], and this in-source reduction (ISR) was subsequently used to sequence disulfide-linked tryptic peptides resulting from digestion of non-reduced serum albumin [15]. It is instructive to note that these previous reports of ISR utilized Fourier transform ion cyclotron resonance and Orbitrap mass spectrometers, while this study employs a quadrupole time-of-flight MS. All three instruments come from different vendors; thus, we can infer that the ISR phenomenon is independent of ESI source setup and MS detection systems.

Clemmer and coworkers have shown that IM can distinguish between OT conformers containing the Cys⁶-Pro⁷ bond in either a *cis*- or *trans*-configuration [38]. It seems reasonable to postulate that the mobilities of disulfide-intact (OT_{SS}) and disulfide-reduced (OT_{SH}) oxytocin would also be distinct, despite the ATDs of Fig. 1 appearing highly similar. We hypothesized that if the changes observed in the OT mass spectra were indeed due to ISR, it should be possible to monitor the relative population of reduced peptide across the arrival time peak. Isotope modeling was employed (see the “Experiment” section) to decompose the experimental mass spectra resulting from scans at the front and tail of the OT peak in the ATD into the contributing populations of OT_{SS} and OT_{SH} (Fig. 2). As mentioned above, and seen in Fig. 1, at neutral pH, the mass spectra at various capillary voltages are indistinguishable; we therefore focused on OT sprayed from acidic solution. At 2 kV, the mass spectra obtained for OT arrival times of 3.88 and 4.02 ms are highly similar, and the isotope modeling indicates that the peptide is ~100% in the OT_{SS} state (Fig. 2a, b). When the voltage is increased to 4 kV, some ISR is observed in the spectrum at 3.88 ms (Fig. 2c) while the amount of disulfide reduction at 4.02 ms is significantly higher, with only ~47% of the peptide remaining in the OT_{SS} state (Fig. 2d).

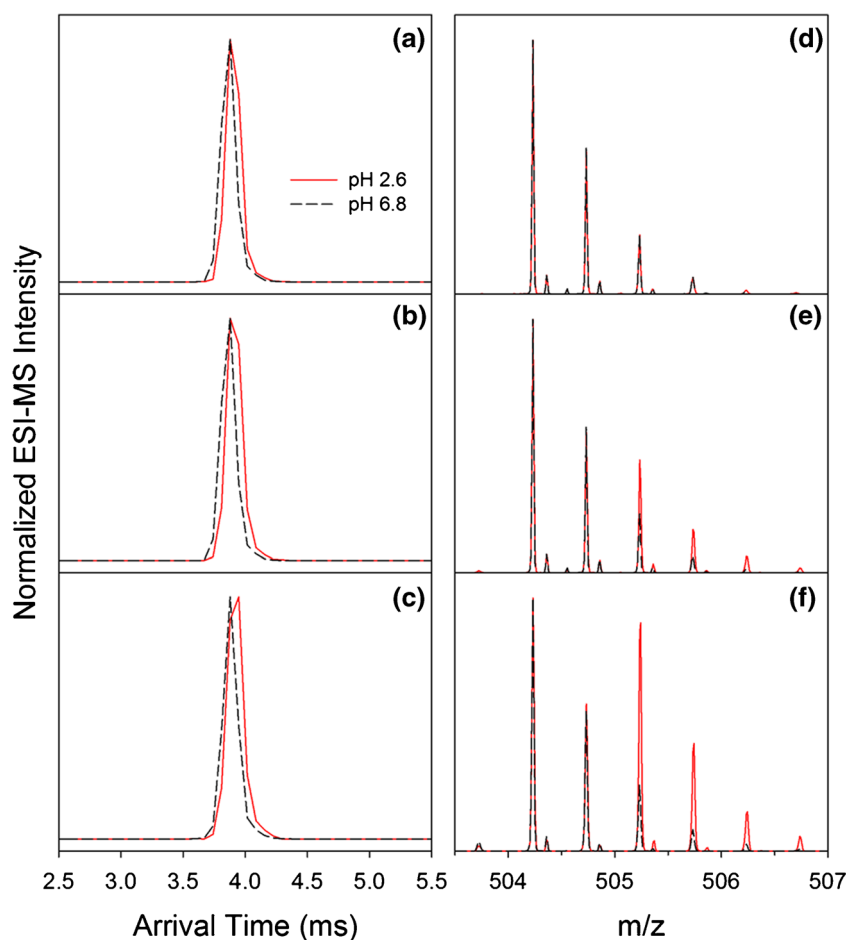


Figure 1. Effects of pH and ESI capillary voltage on oxytocin monitored by ion mobility mass spectrometry. Doubly charged oxytocin arrival time distributions and mass spectra measured at capillary voltages of 2 kV (a, d), 3 kV (b, e), and 4 kV (c, f). Red lines represent the spectra obtained for samples in acidic solution while those from neutral solution are depicted as black dashed lines. The data in each panel were normalized internally to the most intense peak in the arrival time distribution or mass spectrum

The possibility exists that the observed reduction occurs in solution and the marked increase in the $M + 2$ isotopologue signal results from enhanced ionization efficiency of the reduced form at elevated capillary voltage. To assess these potential ESI efficiency differences, we chemically reduced OT with DTT at pH 6.8 and 2.6, and compared the MS results to the corresponding mass spectra for native OT acquired under identical conditions. Using peak intensity ratios of the mono-isotopic signals, minimal differences were observed at low pH between OT_{SS} and OT_{SH} electrosprayed both at 2.5 and 3.5 kV (Fig. S4). Additionally, only marginal ionization efficiency differences were detected for OT_{SH} when comparing intensity ratios from acidic and neutral solutions (Fig. S4). The data presented in Fig. S4 solidify the proposition that the observed disulfide reduction (Fig. 1) is occurring during ionization and not in bulk solution prior to electrospray.

Insulin ISR Observed by IM-MS

To further support the claim of ISR under our ESI conditions, we decided to investigate the heterodimeric peptide insulin. Its two peptide chains, A and B, are connected by two *inter*-chain

disulfide bonds with a third *intra*-chain disulfide located on the A-chain (Fig. S5) [39]. The occurrence of significant ISR should result in an appearance of isolated A- and B-chains in the mass spectrum, and this is exactly what is observed when insulin is electrosprayed from acidic solution at elevated ESI voltages (Fig. S6). We should note however, that under our conditions, only a small amount of molecules undergo complete ISR as the $[\text{insulin} + 5H^+]^{5+}$ peak remains the dominant species in the spectrum (Fig. S7). With the knowledge that insulin was being reduced during ESI, we examined whether IM-MS could be an informative reporter for the onset of ISR.

Figure 3 shows the ATDs (Fig. 3a, b) and corresponding mass spectra (Fig. 3c, d) for $[\text{insulin} + 5H^+]^{5+}$ ionized from different solution conditions at two different ESI capillary voltages. The ATDs obtained at 2.5 kV from neutral and acidic solutions are both dominated by a peak around 6.7 ms (Fig. 3a); however, under low pH conditions, a small shoulder appears at 7.5 ms, indicative of a more extended conformer. The corresponding mass spectrum in Fig. 3c is shifted slightly to higher m/z relative to that acquired from neutral solution. This situation is exacerbated when the ESI capillary is increased to 3.5 kV. The conformer at 7.5 ms is nearly as intense as the

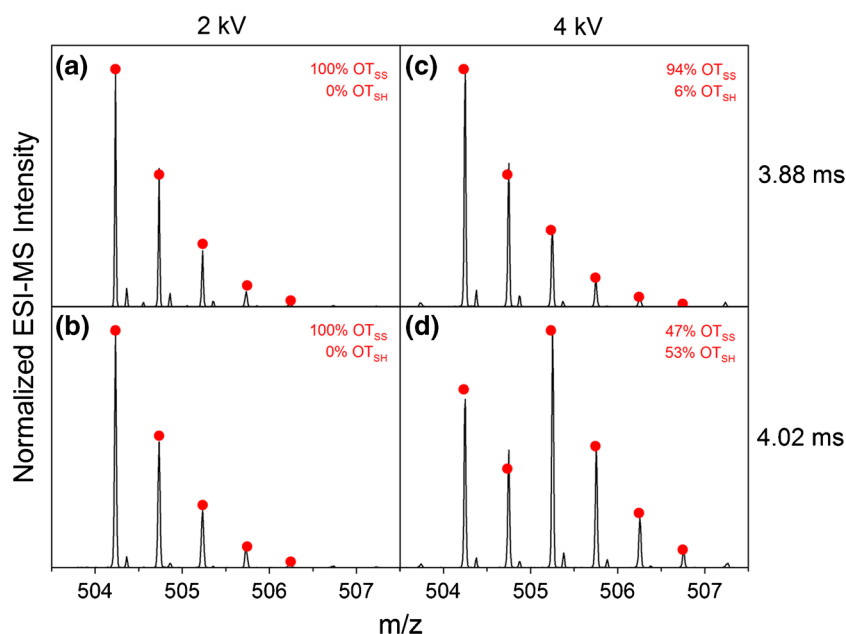


Figure 2. Arrival time-dependent mass spectra of doubly charged oxytocin originating from acidic solution and an ESI capillary voltage of 2 kV (**a, b**) or 4 kV (**c, d**). Spectra were extracted from arrival times of 3.88 ms (**a, c**) and 4.02 ms (**b, d**). Red circles result from isotope modeling (see the “[Experiment](#)” section). Percentages of disulfide-bonded and disulfide-reduced forms of oxytocin are averages of calculations from three replicate samples, and standard deviations are less than 2.5%

6.7 ms species and a third, more extended conformer is populated around 8.3 ms (Fig. 3b). The mass spectrum of the entire low pH ATD is again only shifted a small amount to higher m/z relative to the spectrum from neutral pH (Fig. 3d). However, mass spectra and isotope modeling of the IM-separated conformers reveal a dramatic difference in their disulfide bond characteristics (Fig. S8). Additionally, the 4+ and 5+ charge states exhibit highly similar levels of native insulin (three

disulfides), whereas enhanced disulfide reduction is observed for the 6+ charge state (Fig. S9). These results suggest that there may be a charge state threshold whereupon crossing disulfide ISR becomes more facile.

The ATD we observed for insulin after ISR comprised multiple conformers, similar to measurements on partially reduced states of the disulfide-containing alpha defensin 5 peptide [40]. We can therefore simplify subsequent

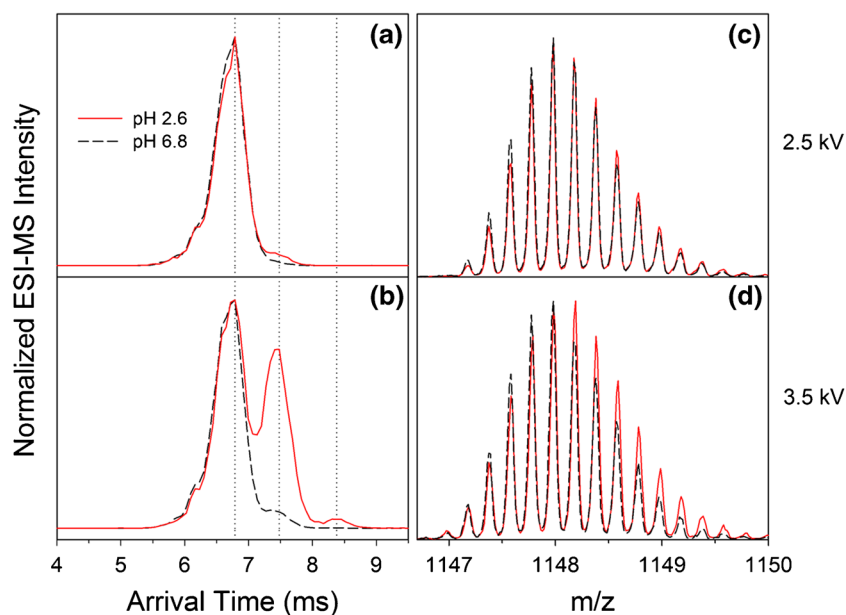


Figure 3. Arrival time distributions and extracted mass spectra for the insulin 5+ charge state, measured at capillary voltages of 2.5 kV (**a, c**) and 3.5 kV (**b, d**). Red and black traces correspond to the peptide samples infused from pH 2.6 and pH 6.8 solutions, respectively. Vertical dotted lines represent the peak maxima of the three conformers in **b** at 6.79, 7.48, and 8.31 ms

discussions by referring to the average arrival time, $\langle t_A \rangle$, calculated as [27]

$$\langle t_A \rangle = \frac{\int I(t_A) t_A dt_A}{\int I(t_A) dt_A} \quad (1)$$

where $I(t_A)$ is the intensity profile of each given arrival time distribution (Fig. 3). The appearance of the A- and B-chains in the mass spectrum obtained at low pH indicates the onset of insulin ISR. Figure 4 shows that after an initial lag phase, the respective intensities for the two chains increase in a nearly linear fashion from 2.5 to 3.5 kV. The plateaus observed for the A-chain (above 3.5 kV) and the B-chain (above 4 kV) likely result from peptide fragmentation in the electrospray source. The discrepancies in MS intensities between the A- and B-chains are not unexpected due to the additional intra-chain disulfide bond within the A-chain; however, differences in ionization efficiency may also play a role. In a similar manner to the isolated chain intensities, the average arrival time at low pH increases dramatically in the range of 2.5–4 kV. In the neutral solution where no ISR is detected, $\langle t_A \rangle$ remains relatively stable (within ~ 0.1 ms) over the entire range of capillary voltages tested (Fig. 4), and the shallow slope is likely due to some conformational activation at elevated voltages. These data underline the utility of IM-MS to detect ISR of disulfide-containing peptides, especially in the case of high charge states ($z \geq 3$) where small shifts in the isotopic envelope may be inconspicuous.

The role of corona discharge in disulfide cleavage has been reported [41], and previous observations of ISR were made at elevated electrospray voltages [13, 15] where corona discharge is known to occur [16, 17]. The pH dependence of ISR observed for oxytocin, and corroborated by the insulin experiments, is a novel finding and suggests a potential

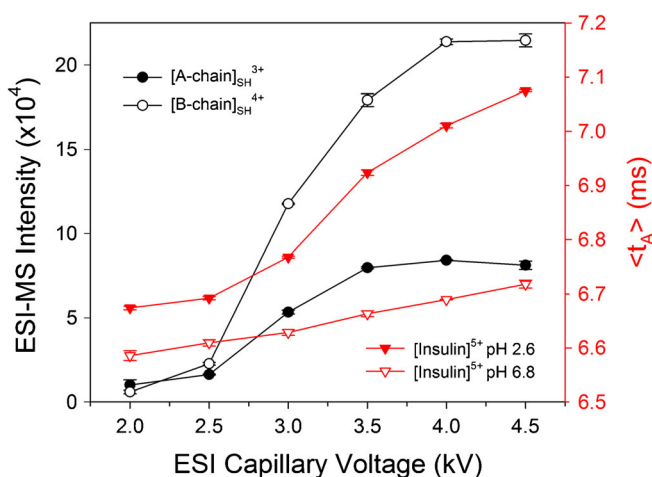


Figure 4. Changes to insulin chain linkage and gas-phase conformation with increasing ESI capillary voltage. *left axis* Intensities of fully reduced insulin A-chain (black circles) and B-chain (open circle) when electrosprayed from acidic solution. *right axis* Average arrival time for the insulin 5+ charge state when arising from acidic (filled triangles) and neutral (open triangles) solutions

electrochemical component to the phenomenon [13]. While the effects of solvent conditions have previously been shown to affect the magnitude of analyte reduction during positive-mode ESI [42], we cannot discount the possible contribution of corona discharge to the disulfide ISR observed here under low pH conditions. A detailed investigation into the mechanism of ISR is beyond the scope of this article, yet we endeavored to uncover whether it could be the cause of a confounding result in the literature concerning the conformational distribution of the highly disulfide-bonded peptide hepcidin [33].

IM-MS Reveals Heparin Compaction Upon ISR

The peptide hormone hepcidin plays a key regulatory role in iron homeostasis by downregulating transport activity of the iron export protein, ferroportin [43], in addition to exhibiting antimicrobial activity [44]. The main isoform, hepcidin-25, is a 25-residue peptide (MW ~ 2.8 kDa) containing four disulfide bonds which folds into a β -hairpin (Fig. S10) [34]. Recent work showed that synthetic hepcidin procured from two separate suppliers resulted in identical LC-MS behavior but remarkably different ATDs [33]. The authors speculate that the different synthetic pathways utilized by the suppliers caused a difference in peptide folding. Differences in higher-order structure must be considered when preparing certified reference materials, and IM-MS has proven useful in delineating the conformational ensemble in growth hormone reference standards [32]. With our knowledge of solution and ESI conditions under which disulfide ISR is observed, we used IM-MS to investigate whether ISR could be the cause of the disparate hepcidin ATDs reported in the literature [33].

As seen for insulin, the measured hepcidin ATDs highlight the importance of solution conditions to the onset of ISR (Fig. 5). When hepcidin is electrosprayed from neutral solution with low ESI voltage, the corresponding ATD for the 3+ charge state exhibits three distinct peaks. The distribution is dominated by an extended species at 6.79 ms with more compact conformers at 6.23 and 5.26 ms. At low capillary voltage, no differences are observed between neutral and low pH solutions (Fig. 5a, b). Dramatic reduction in $\langle t_A \rangle$ in the presence of acid is easily identifiable at 3 kV (Fig. 5c, d), and this shift is further exacerbated by increasing the capillary voltage to 4 kV (Fig. 5e, f), typically at the high end of the voltage range used for most MS experiments. Interestingly, a small decrease in $\langle t_A \rangle$ is also observed when hepcidin is ionized from neutral solution at 4 kV (Fig. 5e). This effect was not observed for oxytocin, and for insulin only to a small extent, but suggests that corona discharge alone may create conditions amenable for partial ISR of some peptides.

We employed isotope modeling to decompose the hepcidin mass spectra into their contributing disulfide forms. Figure 6 shows the experimental m/z isotopic envelopes and corresponding ATDs for the hepcidin 3+ charge state electrosprayed at 3.25 kV from both neutral and low pH solutions. As hepcidin natively contains four disulfide linkages, we report the fraction containing four disulfides, f_{4S-S} , as a measure of ISR. At neutral

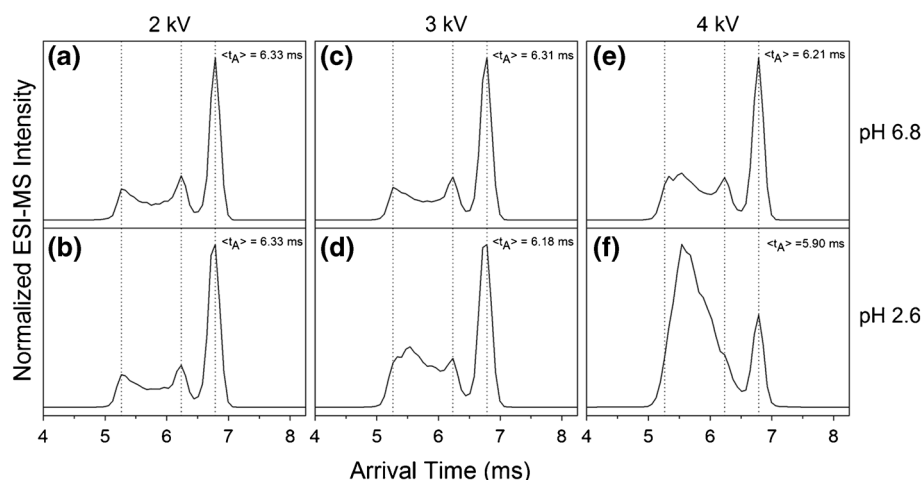


Figure 5. Arrival time distributions for the 3+ hepcidin charge state. Samples were infused from neutral (**a, c, e**) or acidic (**b, d, f**) solutions. Distributions were acquired at capillary voltages of 2 kV (**a, b**), 3 kV (**c, d**), and 4 kV (**e, f**). Dotted lines represent the peak maxima of the three conformers in **a** at 5.26, 6.23, and 6.79 ms. Average arrival times, $\langle t_A \rangle$, were calculated with Eq. (1)

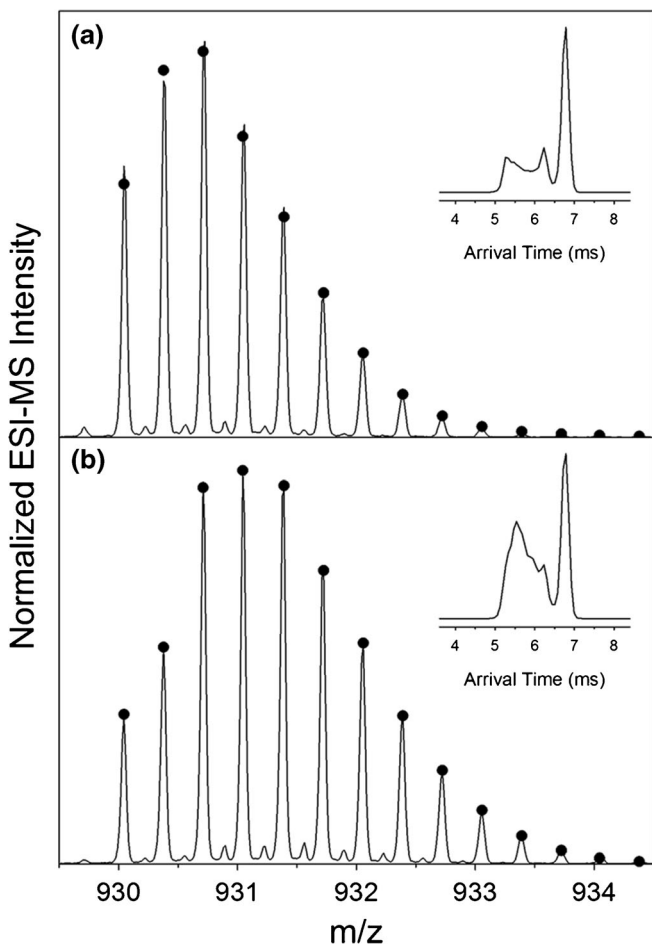


Figure 6. Mass spectra of the hepcidin 3+ charge state acquired at a capillary voltage of 3.25 kV. Peptide solutions were prepared in (**a**) pH 6.8 or (**b**) pH 2.6 solution. Insets depict the associated arrival time distribution for the entire m/z envelope. Black circles are the modeling result for the combination of isotope distributions for hepcidin peptides containing 0–4 disulfide bonds (see the “Experiment” section)

pH (Fig. 6a), the ATD is again dominated by the 6.79-ms peak and an f_{4S-S} of 0.96 indicates that nearly all of the peptide is in its fully disulfide-bonded form. This ATD is highly similar to one reported previously by Bros et al. for hepcidin electro sprayed at 3 kV from an 80:20 solution of water:acetonitrile [33]. The situation is very different when low pH solution is analyzed (Fig. 6b). The ATD still contains the 6.79-ms species; however, a large increase in the intensity of more compact conformers is observed. This distribution exhibits significant resemblance to that obtained by Bros et al. for hepcidin from an alternative supplier, again electro sprayed from 20% ACN at 3 kV [33]. Isotope modeling results in an f_{4S-S} of only 0.66, a ~30% decrease in the native form compared to the neutral solution. While the percentage of organic modifier in the solvent can have an effect on the amount of ISR [15], the results shown here, and in Fig. S11, reinforce the notion that the presence of acid is a key factor. This is analogous to ESI-MS of carotenoids, where analysis of a neutral solution results in the radical molecular ion as the dominant species, whereas ionization from acidic solution leads to detection of mainly the protonated molecule [45].

A complete picture of how disulfide bonding states of hepcidin affect its ATD is depicted in Fig. 7. Figure 7a relates how $\langle t_A \rangle$ of hepcidin decreases with increasing ESI capillary voltage. While the curves at neutral and acidic pH are both sigmoidal with an inflection point around 3.25 kV, the magnitude of the decrease is markedly larger for acidic solution. This trend is mirrored somewhat when plotting f_{4S-S} against ESI voltage (Fig. 7b). At 2 kV, nearly 100% of the hepcidin in neutral solution contain all four disulfide bonds, and this decreases only to 87% at 4 kV. When sprayed from acidic solution at 2 kV, all of the hepcidin is again in its fully disulfide-bonded form. This continues to be the case until the ESI capillary exceeds 2.5 kV, after which there is a steep decrease in f_{4S-S} culminating at 0.33 at 4 kV. The isotope modeling results show that f_{3S-S} increases rapidly after 3 kV

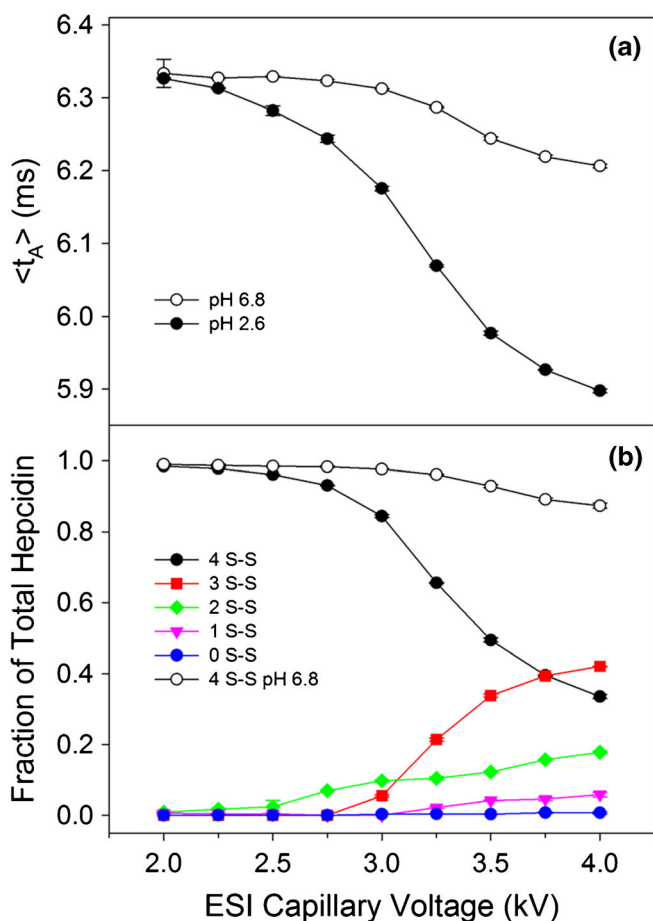


Figure 7. (a) Average arrival time, $\langle t_A \rangle$, of the 3+ hepcidin charge state when electrosprayed from neutral (open circles) and acidic (filled circles) solutions. (b) Fraction of various disulfide-bonding states (0–4 disulfides) calculated from the isotopic envelopes of the hepcidin 3+ charge state when infused from acidic solution (filled symbols). The fraction of fully disulfide-bonded hepcidin (f_{4SS}) present when sprayed from neutral solution is included for comparison (open circles). Error bars represent the standard deviations of triplicate measurements

before beginning to plateau around 0.4 at 4 kV, and f_{2S-S} increases in a slow linear fashion up to 0.2 between 2.5 and 4 kV. Hecpidin molecules with one intact disulfide bond accumulate slightly at elevated voltages; however, fully reduced peptides are not detected to an appreciable extent. Akin to the insulin analysis, we performed isotope modeling on all detectable charge states; however, for hepcidin, there was no obvious charge state effect on the extent of disulfide reduction (Fig. S12). The discrepancy between the two peptides may stem from the nature of the disulfide bonding: hepcidin contains all intra-chain bonds, whereas insulin contains inter-chain linkages in addition to one intra-chain bond. ISR of an insulin inter-chain disulfide would allow for conformational extension, reducing charge repulsion experienced by high protonation states; as a single-chain peptide, this relaxation avenue is not afforded to hepcidin. Sequence effects, i.e., the nature of Cys-flanking residues and total number of basic sites, may also be

playing a role in whether disulfide ISR exhibits a dependence on charge state.

Partial reduction of disulfides in the ESI source results in gas-phase compaction of hepcidin relative to its fully oxidized form (Figs. 5 and 7), the opposite of what is observed for insulin (Fig. 3) and a similarly sized alpha-defensin peptide with 3 disulfide bonds [40]. Gas-phase compaction is a commonly observed event for biomolecules [46], especially those that are non-globular and/or partially extended [26]. Given the conformational restraint provided by the remaining disulfides, it seems plausible that partially reduced hepcidin cannot extend greatly in the gas phase. Interestingly, the ATD for chemically reduced hepcidin indicates a structure only slightly more extended than the fully disulfide-bonded form (Fig. S13). From our findings, it appears reasonable to propose that the dramatic hepcidin mobility differences observed by Bros et al. [33] result from a mixture of partially disulfide-bonded forms. This is ostensibly due to disulfide bond ISR, likely enhanced by different levels of residual acid in the lyophilized peptides resulting in variable solution pH upon reconstitution.

Conclusions

We demonstrated that IM-MS is a useful technique to screen solvent conditions and electrospray parameters that contribute to peptide ISR. This approach is especially valuable for large, highly charged peptides with complex disulfide-bonding patterns where the subtle changes to the isotopic envelope upon partial reduction may go unnoticed. Insulin adopted a more extended gas-phase conformation upon ISR, whereas hepcidin underwent compaction. Ion mobility measurements allowed for facile determination of ISR onset, and decomposition of the hepcidin m/z envelope was afforded by isotope modeling. IM-MS revealed that conformational compaction of hepcidin roughly coincided with the onset of disulfide reduction. Although a previous account invoked corona discharge at elevated ESI voltages as the potential cause of ISR [15], the strong dependence on solution pH observed in this study lends credence to the idea that electrochemistry may be playing a complementary role [13]. Electrochemical reactions are known to occur at the interface of the metal spray capillary and the analyte solution during ESI [47]; therefore, reduced peptide ISR may be observed using an ESI emitter constructed primarily from non-conductive materials [48].

Comparative experiments should be performed under identical conditions; however, this may not always be assured when analyzing small volumes of reconstituted commercial peptides as the counter-ion amount is often omitted from the product specification sheet. Our study promotes the importance of performing ESI-IM-MS of disulfide-containing peptides under minimally activating instrument conditions, as this may alleviate many concerns associated with solution pH and unwanted ISR. ISR-MS/MS experiments have proven useful in the delineation of complex disulfide patterns through peptide sequencing [15]. Given the results presented herein, hepcidin

could be an attractive test system to explore whether, through fragmentation of mobility-separated conformers, partial ISR provides a measure of disulfide selectivity.

Pure peptide reference materials are required for interlaboratory comparative measurements. Final purity values for peptide reference materials must be corrected for related peptide impurities that contribute to the signal measured by LC-MS/MS amino acid analysis after acid hydrolysis, or by quantitative NMR. Quantitation of these peptide impurities is often based on the chromatographic peak area extracted from the monoisotopic peak in the mass spectrum [49]. The occurrence of disulfide ISR will decrease the abundance of the monoisotopic peak, skewing the envelope to higher m/z and should therefore be acknowledged. Although increasing concentrations of organic modifier can offer some protection against ISR [15], any sequence dependence on ISR efficiency remains unexplored. The presence of sequence-dependent ISR of disulfide bonds would have the potential to affect quantitation of related impurities in peptide reference materials.

References

- Fosgerau, K., Hoffmann, T.: Peptide therapeutics: current status and future directions. *Drug Discovery Today*. **20**, 122–128 (2015)
- Bird, G.H., Madani, N., Perry, A.F., Princiotta, A.M., Supko, J.G., He, X., Gavathiotis, E., Sodroski, J.G., Walensky, L.D.: Hydrocarbon double-stapling remedies the proteolytic instability of a lengthy peptide therapeutic. *Proc. Natl. Acad. Sci. U. S. A.* **107**, 14093–14098 (2010)
- Betz, S.F.: Disulfide bonds and the stability of globular proteins. *Protein Sci.* **2**, 1551–1558 (1993)
- Liu, T., Wang, Y., Luo, X., Li, J., Reed, S.A., Xiao, H., Young, T.S., Schultz, P.G.: Enhancing protein stability with extended disulfide bonds. *Proc. Natl. Acad. Sci. U. S. A.* **113**, 5910–5915 (2016)
- Li, Y., Li, X., Zheng, X., Tang, L., Xu, W., Gong, M.: Disulfide bond prolongs the half-life of therapeutic peptide-GLP-1. *Peptides*. **32**, 1400–1407 (2011)
- Góngora-Benítez, M., Tulla-Puche, J., Albericio, F.: Multifaceted roles of disulfide bonds. Peptides as therapeutics. *Chem. Rev.* **114**, 901–926 (2014)
- Moore, S.J., Leung, C.L., Cochran, J.R.: Knottins: disulfide-bonded therapeutic and diagnostic peptides. *Drug Discovery Today: Technol.* **9**, e1–e11 (2012)
- Gorman, J.J., Wallis, T.P., Pitt, J.J.: Protein disulfide bond determination by mass spectrometry. *Mass Spectrom. Rev.* **21**, 183–216 (2002)
- Xia, Y., Cooks, R.G.: Plasma induced oxidative cleavage of disulfide bonds in polypeptides during nanoelectrospray ionization. *Anal. Chem.* **82**, 2856–2864 (2010)
- Stinson, C.A., Xia, Y.: Radical induced disulfide bond cleavage within peptides via ultraviolet irradiation of an electrospray plume. *Analyst*. **138**, 2840–2846 (2013)
- Mentinova, M., McLuckey, S.A.: Cleavage of multiple disulfide bonds in insulin via gold cationization and collision-induced dissociation. *Int. J. Mass Spectrom.* **308**, 133–136 (2011)
- Kraj, A., Brouwer, H.-J., Reinhoud, N., Chervet, J.-P.: A novel electrochemical method for efficient reduction of disulfide bonds in peptides and proteins prior to MS detection. *Anal. Bioanal. Chem.* **405**, 9311–9320 (2013)
- Nicolardi, S., Deelder, A.M., Palmblad, M., van der Burgt, Y.E.: Structural analysis of an intact monoclonal antibody by online electrochemical reduction of disulfide bonds and Fourier transform ion cyclotron resonance mass spectrometry. *Anal. Chem.* **86**, 5376–5382 (2014)
- Trabjerg, E., Jakobsen, R.U., Mysling, S., Christensen, S., Jørgensen, T.J.D., Rand, K.D.: Conformational analysis of large and highly disulfide-stabilized proteins by integrating online electrochemical reduction into an optimized H/D exchange mass spectrometry workflow. *Anal. Chem.* **87**, 8880–8888 (2015)
- Cramer, C.N., Kelstrup, C.D., Olsen, J.V., Haselmann, K.F., Nielsen, P.K.: Complete mapping of complex disulfide patterns with closely-spaced cysteines by in-source reduction and data-dependent mass spectrometry. *Anal. Chem.* **89**, 5949–5957 (2017)
- Morand, K., Talbo, G., Mann, M.: Oxidation of peptides during electrospray ionization. *Rapid Commun. Mass Spectrom.* **7**, 738–743 (1993)
- Boys, B.L., Kuprowski, M.C., Konermann, L.: Protein oxidative modifications during electrospray ionization: solution phase electrochemistry or corona discharge-induced radical attack? *Anal. Chem.* **81**, 4027–4034 (2009)
- Koeniger, S.L., Merenbloom, S.I., Clemmer, D.E.: Evidence for many resolvable structures within conformation types of electrosprayed ubiquitin ions. *J. Phys. Chem. B.* **110**, 7017–7021 (2006)
- Scarf, C.A., Patel, V.J., Thalassinou, K., Scrivens, J.H.: Probing hemoglobin structure by means of traveling-wave ion mobility mass spectrometry. *J. Am. Soc. Mass Spectrom.* **20**, 625–631 (2009)
- Knapman, T.W., Morton, V.L., Stonehouse, N.J., Stockley, P.G., Ashcroft, A.E.: Determining the topology of virus assembly intermediates using ion mobility spectrometry-mass spectrometry. *Rapid Commun. Mass Spectrom.* **24**, 3033–3042 (2010)
- Bleiholder, C., Dupuis, N.F., Wyttenbach, T., Bowers, M.T.: Ion mobility-mass spectrometry reveals a conformational conversion from random assembly to β -sheet in amyloid fibril formation. *Nat. Chem.* **3**, 172–177 (2011)
- Seo, J., Hoffman, W., Warmke, S., Bowers, M.T., Pagel, K., von Helden, G.: Retention of native protein structures in the absence of solvent: a coupled ion mobility and spectroscopic study. *Angew. Chem. Int. Ed.* **55**, 14173–14176 (2016)
- Göth, M., Pagel, K.: Ion mobility-mass spectrometry as a tool to investigate protein-ligand interactions. *Anal. Bioanal. Chem.* **409**, 4305–4310 (2017)
- Pacholarz, K.J., Burnley, R.J., Jowitt, T.A., Ordsmith, V., Pisco, J.P., Porrini, M., Larrouy-Maumus, G., Garlish, R.A., Taylor, R.J., de Carvalho, L.P., Barran, P.E.: Hybrid mass spectrometry approaches to determine how L-histidine feedback regulates the enzyme MtATP-phosphoribosyltransferase. *Structure*. **25**, 730–738 (2017)
- Ruotolo, B.T., Robinson, C.V.: Aspects of native proteins are retained in vacuum. *Curr. Opin. Chem. Biol.* **10**, 402–408 (2006)
- Devine, P.W.A., Fisher, H.C., Calabrese, A.N., Whelan, F., Higazi, D.R., Potts, J.R., Lowe, D.C., Radford, S.E., Ashcroft, A.E.: Investigating the structural compaction of biomolecules upon transition to the gas-phase using ESI-TWIMS-MS. *J. Am. Soc. Mass Spectrom.* **28**, 1855–1862 (2017)
- Vahidi, S., Stocks, B.B., Konermann, L.: Partially disordered proteins studied by ion mobility-mass spectrometry: implications for the preservation of solution phase structure in the gas phase. *Anal. Chem.* **85**, 10471–10478 (2013)
- Distler, U., Kuharev, J., Navarro, P., Levin, Y., Schild, H., Tenzer, S.: Drift time-specific collision energies enable deep-coverage data-independent acquisition proteomics. *Nat. Methods*. **11**, 167–170 (2014)
- Pierson, N.A., Chen, L., Valentine, S.J., Russell, D.H., Clemmer, D.E.: Number of solution states of bradykinin from ion mobility and mass spectrometry measurements. *J. Am. Chem. Soc.* **133**, 13810–13813 (2011)
- Pierson, N.A., Chen, L., Russell, D.H., Clemmer, D.E.: *Cis-trans* isomerizations of proline residues are key to bradykinin conformations. *J. Am. Chem. Soc.* **135**, 3186–3192 (2013)
- Massonnet, P., Haler, J.R.N., Upert, G., Degueldre, M., Morsa, D., Smargiasso, N., Mourier, G., Gilles, N., Quinton, L., De Pauw, E.: Ion mobility-mass spectrometry as a tool for the structural characterization of peptides bearing intramolecular disulfide bond(s). *J. Am. Soc. Mass Spectrom.* **27**, 1637–1646 (2016)
- Pritchard, C., O'Connor, G., Ashcroft, A.E.: The role of ion mobility spectrometry-mass spectrometry in the analysis of protein reference standards. *Anal. Chem.* **85**, 7205–7212 (2013)
- Bros, P., Josephs, R.D., Stoppacher, N., Cazals, G., Lehmann, S., Hirtz, C., Wielgosz, R.I., Delatour, V.: Impurity determination for hepcidin by liquid chromatography-high resolution and ion mobility mass spectrometry for the value assignment of candidate primary calibrators. *Anal. Bioanal. Chem.* **409**, 2559–2567 (2017)

34. Jordan, J.B., Poppe, L., Haniu, M., Arvedson, T., Syed, R., Li, V., Kohno, H., Kim, H., Schnier, P.D., Harvey, T.S., Miranda, L.P., Cheetham, J., Sasu, B.J.: Hepcidin revisited, disulfide connectivity, dynamics, and structure. *J. Biol. Chem.* **284**, 24155–24167 (2009)
35. Bush, M.F., Campuzano, I.D.G., Robinson, C.V.: Ion mobility mass spectrometry of peptide ions: effects of drift gas and calibration strategies. *Anal. Chem.* **84**, 7124–7130 (2012)
36. Chalkley, R.J., Baker, P.R., Medzihradzky, K.F., Lynn, A.J., Burlingame, A.L.: In-depth analysis of tandem mass spectrometry data from disparate instrument types. *Mol. Cell. Proteomics.* **7**, 2386–2398 (2008)
37. Koehbach, J., O'Brien, M., Muttenthaler, M., Miazzo, M., Akcan, M., Elliott, A.G., Daly, N.L., Harvey, P.J., Arrowsmith, S., Gunasekera, S., Smith, T.J., Wray, S., Göransson, U., Dawson, P.E., Craik, D.J., Freissmuth, M., Gruber, C.W.: Oxytocic plant cyclotides as templates for peptide G protein-coupled receptor ligand design. *Proc. Natl. Acad. Sci. U. S. A.* **110**, 21183–21188 (2013)
38. Fuller, D.R., Glover, M.S., Pierson, N.A., Kim, D., Russell, D.H., Clemmer, D.E.: Cis→trans isomerization of Pro(7) in oxytocin regulates Zn(2+) binding. *J. Am. Soc. Mass Spectrom.* **27**, 1376–1382 (2016)
39. Ryle, A.P., Sanger, F., Smith, L.F., Kitai, R.: The disulphide bonds of insulin. *Biochem. J.* **60**, 541–556 (1955)
40. Snijder, J., van de Waterbeemd, M., Glover, M.S., Shi, L., Clemmer, D.E., Heck, A.J.: Conformational landscape and pathway of disulfide bond reduction of human alpha defensin. *Protein Sci.* **24**, 1264–1271 (2015)
41. Li, G., Pei, J., Yin, Y., Huang, G.: Direct sequencing of a disulfide-linked peptide with electrospray ionization tandem mass spectrometry. *Analyst.* **140**, 2623–2627 (2015)
42. Gianelli, L., Amendola, V., Fabbrizzi, L., Pallavicini, P., Mellerio, G.G.: Investigation of reduction of Cu(II) complexes in positive-ion mode electrospray mass spectrometry. *Rapid Commun. Mass Spectrom.* **15**, 2347–2353 (2001)
43. Nemeth, E., Tuttle, M.S., Powelson, J., Vaughn, M.B., Donovan, A., McVey Ward, D., Ganz, T., Kaplan, J.: Hepcidin regulates cellular iron efflux by binding to ferroportin and inducing its internalization. *Science.* **306**, 2090–2093 (2004)
44. Krause, A., Neitz, S., Mägert, H.-J., Schulz, A., Forssmann, W.-G., Schulz-Knappe, P., Adermann, K.: LEAP-1, a novel highly disulfide-bonded human peptide, exhibits antimicrobial activity. *FEBS Lett.* **480**, 147–150 (2000)
45. Guaratini, T., Gates, P.J., Pinto, E., Colepicolo, P., Lopes, N.P.: Differential ionisation of natural antioxidant polyenes in electrospray and nanospray mass spectrometry. *Rapid Commun. Mass Spectrom.* **21**, 3842–3848 (2007)
46. Pagel, K., Natan, E., Hall, Z., Fersht, A.R., Robinson, C.V.: Intrinsically disordered p53 and its complexes populate compact conformations in the gas phase. *Angew. Chem. Int. Ed.* **52**, 361–365 (2013)
47. Abonnenc, M., Qiao, L., Liu, B., Girault, H.H.: Electrochemical aspects of electrospray and laser desorption/ionization for mass spectrometry. *Annu. Rev. Anal. Chem.* **3**, 231–254 (2010)
48. Zinck, N., Stark, A.K., Wilson, D.J., Sharon, M.: An improved rapid mixing device for time-resolved electrospray mass spectrometry measurements. *Chemistry Open.* **3**, 109–114 (2014)
49. Stoppacher, N., Josephs, R.D., Daireaux, A., Choteau, T., Westwood, S., Wielgosz, R.I.: Accurate quantification of impurities in pure peptide material—angiotensin I: comparison of calibration requirements and method performance characteristics of liquid chromatography coupled to hybrid tandem mass spectrometry and linear ion trap high-resolution mass spectrometry. *Rapid Commun. Mass Spectrom.* **29**, 1651–1660 (2015)